J Appl Physiol 104: 1743–1752, 2008.
First published March 20, 2008; doi:10.1152/japplphysiol.01355.2007.

Effect of heterogeneous ventilation and nitric oxide production on exhaled nitric oxide profiles

Vinod Suresh,[1]* David A. Shelley,[2]* Hye-Won Shin,[1] and Steven C. George[1,2]

[1]*Department of Biomedical Engineering and* [2]*Department of Chemical Engineering and Materials Science, University of California, Irvine, Irvine, California*

Submitted 20 December 2007; accepted in final form 10 March 2008

Suresh V, Shelley DA, Shin H-W, George SC. Effect of heterogeneous ventilation and nitric oxide production on exhaled nitric oxide profiles. *J Appl Physiol* 104: 1743–1752, 2008. First published March 20, 2008; doi:10.1152/japplphysiol.01355.2007.—Elevated exhaled nitric oxide (NO) in the breath of asthmatic subjects is thought to be a noninvasive marker of lung inflammation. Asthma is also characterized by heterogeneous bronchoconstriction and inflammation, which impact the spatial distribution of ventilation in the lungs. Since exhaled NO arises from both airway and alveolar regions, and its level in exhaled breath depends strongly on flow, spatial heterogeneity in flow patterns and NO production may significantly affect the exhaled NO signal. To investigate the effect of these factors on exhaled NO profiles, we developed a multicompartment mathematical model of NO exchange using a trumpet-shaped central airway segment that bifurcates into two similarly shaped peripheral airway segments, each of which empties into an alveolar compartment. Heterogeneity in flow alone has only a minimal impact on the exhaled NO profile. In contrast, placing 70% of the total airway NO production in the central compartment or the distal poorly ventilated compartment can significantly increase (35%) or decrease (−10%) the plateau concentration, respectively. Reduced ventilation of the peripheral and acinar regions of the lungs with concomitant elevated NO production delays the rise of NO during exhalation, resulting in a positive phase III slope and reduced plateau concentration (−11%). These features compare favorably with experimentally observed profiles in exercise-induced asthma and cannot be simulated with single-path models. We conclude that variability in ventilation and NO production in asthmatic subjects impacts the shape of the exhaled NO profile and thus impacts the physiological interpretation.

asthma; inflammation; model; multicompartment

ASTHMA is a pulmonary disorder characterized by chronic airway inflammation and airflow obstruction that is widespread, but variable in space and time. Although airflow obstruction is routinely monitored with spirometry, assessing inflammation in a noninvasive manner is more difficult. The concentration of nitric oxide (NO) is elevated in the exhaled breath of asthmatics and has tremendous potential to be a noninvasive marker of inflammation (1, 11).

NO exchange in the lungs exhibits two distinguishing features that need to be considered for a proper interpretation of the exhaled signal. First, exhaled NO is produced in both the airway and alveolar regions of the lung (18, 20, 28, 30). Second, exhaled NO concentration is highly dependent on the exhalation flow (25, 30). In a disease such as asthma, inflammation and flow are spatially heterogeneous. As a result, the exhaled NO concentration may increase or decrease during the course of an exhalation even when flow is held constant. Thus far, mathematical models of NO exchange dynamics in the lungs have apportioned NO exchange into one airway and one alveolar compartment, each having homogeneous ventilation and NO production (4, 8, 19, 23, 26, 28, 31). Such models effectively simulate the flow dependence of exhaled NO but are unable to describe variations in NO concentration when flow is held constant.

While asthma has traditionally been considered to be a disease of the proximal/conducting airways (generations 0–16), recent studies have indicated significant inflammation of the distal/acinar airways and alveolar regions (generations 17–23) (6, 9, 10, 17). Imaging and multiple-breath washout studies have also demonstrated ventilation defects or heterogeneity in the proximal and distal regions of the lung (7, 32, 33, 35). Furthermore, heterogeneity in flow and NO production are likely consequences of heterogeneous inflammation. This study describes a mathematical model of NO exchange in the lungs that incorporates heterogeneity in ventilation and NO production in both the airway and alveolar regions of the lung. Using the simplest such model, we demonstrate that heterogeneity in ventilation and NO production significantly influences the exhaled NO profile in a pattern consistent with experimental observations in asthma.

Glossary

$A(z)$	Total cross-sectional area of airway compartment at location z (cm^2)
$A_1(z)$	Cross-sectional area of airway *compartment 1* at location z (cm^2)
$A_2(z)$	Cross-sectional area of airway *compartment 2* at location z (cm^2)
$C(z,t)$	Concentration of no in airway compartment at location z and time t (ppb)
$C_{ANO,1}$	Steady-state concentration of no in alveolar *compartment 1* (ppb)
$C_{ANO,2}$	Steady-state concentration of no in alveolar *compartment 2* (ppb)
$\bar{C}A_{NO}$	Volume-weighted average alveolar concentration (ppb)
$Dair_{NO}$	Molecular diffusivity of no in air (cm^2/s)
f	Fraction of total maximum airway flux in *compartment 1*
$FE_{NO,50}$	Plateau fractional concentration of NO at constant exhalation flow of 50 ml/s (ppb)

* V. Suresh and D. A. Shelley contributed equally to this study.

Address for reprint requests and other correspondence: S. C. George, Dept. of Biomedical Engineering, 3120 Natural Sciences II, Univ. of California, Irvine, Irvine, CA 92697-2715 (e-mail: scgeorge@uci.edu).

The costs of publication of this article were defrayed in part by the payment of page charges. The article must therefore be hereby marked "*advertisement*" in accordance with 18 U.S.C. Section 1734 solely to indicate this fact.

$F_{E_{NO,\dot{V}}}$	Fractional concentration of NO in phase III at a constant exhalation flow
FEV_1	Forced expiratory volume in 1 s (%predicted)
FVC	Forced vital capacity (%predicted)
$J'aw_{NO}$	Total maximum airway wall flux of NO (pl/s)
$J'aw_{NO,0}$	Maximum airway wall flux of NO in central airway *compartment 0* (pl/s)
$J'aw_{NO,1}$	Maximum airway wall flux of NO in airway *compartment 1* (pl/s)
$J'aw_{NO,2}$	Maximum airway wall flux of NO in airway *compartment 2* (pl/s)
$\bar{J}'aw_{NO}$	Flow-weighted maximal airway wall flux for the whole airway tree (pl/s)
r	Ratio of steady-state NO concentration in alveolar *compartment 1* to that in alveolar *compartment 2*
$\bar{S}_{III_{N_2}}$	Normalized phase III slope of exhaled nitrogen (dimensionless)
$\bar{S}_{III_{NO}}$	Normalized phase III slope of exhaled NO (dimensionless)
$\bar{S}_{III_{\dot{V}}}$	Normalized phase III slope of exhalation flow (dimensionless)
Sacin	Index of ventilation heterogeneity in acinar airways ($liters^{-1}$)
Scond	Index of ventilation heterogeneity in conducting airways ($liters^{-1}$)
V_A	Total volume of alveolar compartments (ml)
V_{A_1}	Volume of alveolar *compartment 1* (ml)
V_{A_2}	Volume of alveolar *compartment 2* (ml)
Vaw	Total airway volume (ml)
Vaw_0	Volume of airway *compartment 0* (ml)
Vaw_1	Volume of airway *compartment 1* (ml)
Vaw_2	Volume of airway *compartment 2* (ml)
Vex	Volume of air exhaled (ml)
$V90_{NO}$	Normalized exhaled volume of air (number of exhaled airway volumes) required for the exhaled NO concentration to reach 90% of its plateau value (dimensionless)
$\dot{V}$	Total exhalation flow (ml/s)
$\dot{V}_1(t)$	Flow in airway *compartment 1* at time *t* (ml/s)
$\dot{V}_2(t)$	Flow in airway *compartment 1* at time *t* (ml/s)
$\dot{V}_{1,0}$	Initial (*time 0*) flow in *compartment 1* (ml/s)
$\dot{V}_{2,0}$	Initial (*time 0*) flow in *compartment 2* (ml/s)
$\dot{V}_{1,\infty}$	Steady-state flow in *compartment 1* (ml/s)
$\dot{V}_{2,\infty}$	Steady-state flow in *compartment 2* (ml/s)
$\dot{V}_{III}$	Mean exhalation flow during phase III (ml/s)
α	Fraction of the total airway cross-section area at bifurcation point in multicompartment model assigned to *compartment 1*
τ	Characteristic time constant of $\dot{V}_1(t)$ and $\dot{V}_2(t)$ (s)

METHODS

A simple model of the human lung incorporating airway and alveolar heterogeneity in ventilation and NO production was developed. The model consists of a trumpet-shaped central airway compartment (*compartment 0*) which bifurcates into two trumpet-shaped lower airway compartments, *1* and *2* (Fig. 1). Each of the lower compartments empties into a well-mixed alveolar compartment.

Geometry. The model geometry is based on the symmetric bifurcating data of Weibel (38). A continuous airway cross-sectional area $A(z)$ was obtained as a function of the distance z from the oropharynx by interpolating the Weibel data using a piecewise cubic Hermite polynomial. The airway volume at a location z is then given by $Vaw(z)\int_0^z A(s)ds$. The volume of the conducting airways (generations 0–16) in the Weibel model is approximately equal to 175 cm^3. The linear dimension of the Weibel data was scaled by $(181/175)^{1/3}$ to simulate a lung with a total airway volume Vaw = 181 cm^3 that is similar to the group of asthmatic subjects included in this study (see below). For a given subject, Vaw (ml) is fixed at the subject's ideal body weight (pounds) plus age in years (3, 29). The total volume of the alveolar compartments V_A was set equal to 2,500 ml to simulate a typical adult functional residual capacity (FRC).

The central airway compartment incorporates the first N generations of the airway tree with volume Vaw_0. Distal to generation N, the airway tree is split into two compartments characterized by different flow dynamics. Thus the lower airway compartments incorporate the remaining $17 - N$ airway generations, but with different cross sections A_i and volumes Vaw_i ($i = 1,2$), while the alveolar region is

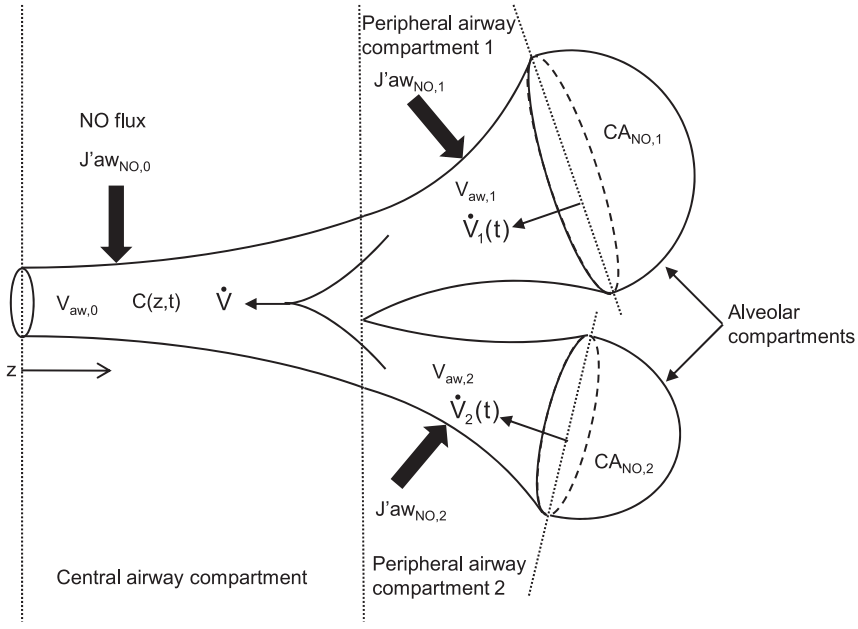

Fig. 1. Schematic of the multicompartment model. A trumpet-shaped central airway compartment bifurcates into 2 peripheral airway compartments, each of which empties into an expansile alveolar region. Each airway compartment has a constant airway wall flux of nitric oxide (NO) per unit volume, and each alveolar compartment has a constant NO concentration. Exhalation flow in the alveolar and peripheral airway compartments are time, and thus volume, dependent, while the net exhalation flow is held constant. NO concentration within the model varies as a function of time and distance z from the mouth. Symbols are defined in *Glossary*.

divided into two compartments with volumes V_{A_1} and V_{A_2} and represents a functional division of the lungs into two regions (one well ventilated and the other poorly ventilated). A fraction α of the total cross-sectional area from the Weibel geometry is assigned to *compartment 1*, and the remainder $(1 - \alpha)$ to *compartment 2* so that $A_1/A_2 = Vaw_1/Vaw_2 = V_{A_1}/V_{A_2} = \alpha/(1 - \alpha)$. The overall length of the airway tree, i.e., the sum of the lengths of *compartment 0* and *compartments 1* or *2*, representing the distance from the oropharynx to the respiratory zone, is equal to that of the Weibel model (appropriately scaled). In this construction, N and α are free structural parameters whose determination is discussed below.

Ventilation. Compartments 1 and *2* are allowed to empty at different time-dependent rates $\dot{V}_1(t)$ and $\dot{V}_2(t)$ with the constraint that the total exhalation flow at the mouth, $\dot{V} = \dot{V}_1(t) + \dot{V}_2(t)$, be constant. This choice makes possible the simulation of constant-flow exhalations commonly used to characterize exhaled NO while simultaneously incorporating the effects of ventilation heterogeneity. Then, the flow in *compartment i* ($i = 1,2$) is given by (2)

$$\dot{V}_i = (\dot{V}_{i,0} - \dot{V}_{i,\infty})e^{-t/\tau} + \dot{V}_{i,\infty} \quad (1)$$

subject to the constraints

$$(\dot{V}_{1,0} - \dot{V}_{1,\infty}) + (\dot{V}_{2,0} - \dot{V}_{2,\infty}) = 0 \quad (2)$$

$$\dot{V}_{1,\infty} + \dot{V}_{2,\infty} = \dot{V} \quad (3)$$

In this analysis the pressures in the two compartments are assumed to be equal during the entire exhalation (2). Here $\dot{V}_{i,0}$ and $\dot{V}_{i,\infty}$ are the initial ($t = 0$) and steady-state or infinite time ($t \to \infty$) flows in *compartment i*, and τ is a characteristic time constant. These parameters can be expressed in terms of airway resistance (R_i) and tissue elastance (E_i) of *compartment i* (2), which, in turn, are related to both the geometry (i.e., constriction status) of the airways and the material properties of lung tissue. Importantly, when the total flow $\dot{V}$ is strictly constant, *compartments 1* and *2* are tightly coupled, and the system is characterized by a single time constant $\tau = (R_1 + R_2)/(E_1 + E_2)$. This provides the most flexible structure that may be useful to simulate diseases other than asthma that may have a larger impact on the interstitial tissue. In the case of asthma, flow heterogeneity can be simulated by setting the elastance of the regions to be equal to each other, and then varying the resistance through each compartment. Thus we assume a constant total elastance (E_T), or $\tau = 2(R_1 + R_2)/(E_T)$, consistent with previous reports simulating flow heterogeneity in asthma (27). Using this structure, it can be shown that $\dot{V}_{1,\infty} = \dot{V}_{2,\infty} = \dot{V}/2$. Hence, we treat $\dot{V}_{1,0}$ and τ as the independent free parameters while $\dot{V}_{2,0}$ is determined from the constraint above (*Eq. 2*). Therefore, the structure and ventilation of the multicompartment model for asthma is characterized by four independent parameters: N, α, $\dot{V}_{1,0}$, and τ.

NO production. NO production is characterized by specifying the steady-state NO concentrations $C_{A_{NO,1}}$ and $C_{A_{NO,2}}$ in the alveolar compartments and the maximum airway wall flux $J'aw_{NO,i}$ in each airway compartment i ($i = 0,1,2$). $J'aw_{NO,i}$ is obtained by using previously published values of the total airway flux (4, 21–24, 26, 31) and partitioning it between compartments in proportion to their volume:

$$J'aw_{NO,i} = \frac{Vaw_i}{Vaw} J'aw_{NO} \quad (4)$$

where $J'aw_{NO} = \sum_{i=0}^{2} J'aw_{NO,i}$. Such a partitioning results in uniform NO production per unit airway volume, and, in combination with the choice $C_{A_{NO,1}} = C_{A_{NO,2}}$, is used to simulate a lung with homogeneous NO production.

Heterogeneous NO production is simulated in three different ways: *1*) the airway flux in one of the compartments is specified to be a fraction f of the total flux, and the remaining fraction $(1 - f)$ is partitioned equally between the other two compartments in proportion to their volume; *2*) specifying a ratio r of alveolar NO concentrations ($r \neq 1$), $C_{A_{NO,1}} = r \times C_{A_{NO,2}}$, but maintaining a constant volume-weighted alveolar concentration ($C_{A_{NO}} = C_{A_{NO,1}} \times V_{A_1}/V_A + C_{A_{NO,2}} \times V_{A_2}/VA$); or *3*) a combination of *1* and *2*. Thus, for these simulations, NO production is specified by two free parameters ($J'aw_{NO}$, $C_{A_{NO}}$) in the homogeneous case and four free parameters ($J'aw_{NO}$, f, $C_{A_{NO}}$, r) in the heterogeneous case.

Governing equations. The concentration of NO, $C(t,z)$, at time t and axial location z within each compartment is governed by the following convection-diffusion equation (4, 23):

$$\frac{\partial C}{\partial t} + \frac{\dot{V}_i(t)}{A_i(z)}\frac{\partial C}{\partial z} = \frac{D}{A_i(z)}\frac{\partial}{\partial z}\left(A_i(z)\frac{\partial C}{\partial z}\right) + \frac{J'aw_{NO,i}}{Vaw_i} \quad (5)$$

with $i = 0,1,2$. Initial and boundary conditions are given by

$$\begin{aligned} &C(0,z) = 0 \\ &\frac{\partial C}{\partial z} = 0 \text{ at } z = 0 \text{ (mouth)} \\ &C = C_{A_{NO,1}} \text{ at } z = z_{17} \\ &C = C_{A_{NO,2}} \text{ at } z = z_{17} \end{aligned} \quad (6)$$

where z_{17} represents the location of the alveolar-terminal bronchiole interface situated at the distal end of generation 17 in the Weibel model. A fully time-implicit scheme with upwinding for the convective term was used to discretize the convection-diffusion equation. Conservation of mass at the intersection of *compartments 0, 1,* and *2* was enforced by performing a mass balance over a control volume surrounding the intersection point, leading to the following relationship:

$$V\frac{dC_{N_0}}{dt} = (\dot{V}C_{N_0-1} - \dot{V}_1 C_{N_0+1} - \dot{V}_2 C_{N_0+N_1+1}) - D\left(A_{N_0-1}\frac{\partial C}{\partial z}\bigg|_{N_0-1} - A_{N_0+1}\frac{\partial C}{\partial z}\bigg|_{N_0+1} - A_{N_0+N_1+1}\frac{\partial C}{\partial z}\bigg|_{N_0+N_1+1}\right) + J'_{N_0} \quad (7)$$

where C_i is the concentration at discretization point i, V is the volume of the control volume, and J'_{N_0} is the total wall flux in the control volume.

Multiple-breath nitrogen washout. Multiple-breath nitrogen washout (MBNW) is a lung function test used to examine ventilation heterogeneity in the proximal and peripheral airways (12, 14, 15, 35). Briefly, patients tidal-breathe pure O_2, and the exhaled concentration of nitrogen is measured, tracking the nitrogen washout from the lungs (Fig. 2*A*). The normalized phase III slope for nitrogen is positive and progressively increases with each tidal breath (Fig. 2*B*). The phase III slope of each exhalation is normalized by the mean concentration of the gas over the region of analysis (typically 50–90% of the exhaled volume). Plotting the normalized phase III slope of nitrogen ($\bar{S}_{III_{N_2}}$) as a function of functional residual capacity turnover (cumulative exhaled volume divided by functional residual capacity) allows quantification of regional ventilation heterogeneity.

Models have been presented that show that $\bar{S}_{III_{N_2}}$ for early breath numbers is controlled by diffusion and convection-dependent inhomogeneities (DCDI), while $\bar{S}_{III_{N_2}}$ for later breath numbers is controlled by convection-dependent inhomogeneities (CDI) (13–16, 34, 37). These models have been used to explain how the two distinct segments of the $\bar{S}_{III_{N_2}}$ plot represent inhomogeneities in different regions of the lung. Sacin is an index of ventilation inhomogeneity in the acinar airways, while Scond is an index of inhomogeneity in the conducting airways (see schematic in Fig. 2*C*).

We first utilize the multicompartment model to simulate the exchange of nitrogen during a MBNW in order to determine model structural and ventilation parameters independent of the NO exchange parameters. The governing equation is identical to the NO exchange equation (*Eq. 5*) except the source term is removed. At the start of the washout, the fractional nitrogen concentration in the model is uniform

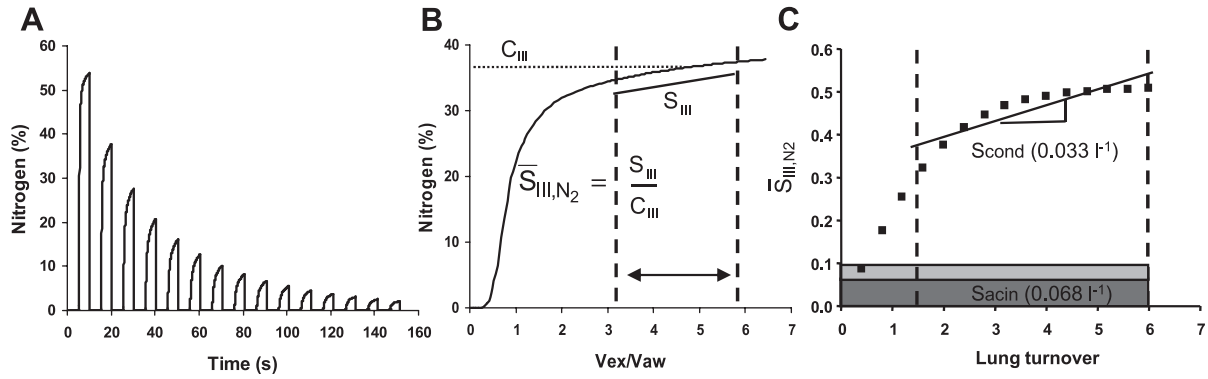

Fig. 2. Simulation of multiple-breath nitrogen washout for a healthy subject. *A*: typical profiles showing the washout of nitrogen from the lungs during tidal breathing of 100% oxygen. The fractional nitrogen concentration in exhaled air is plotted a function of time. *B*: determination of normalized phase III slope ($S_{III_{N_2}}$). Simulated exhaled nitrogen concentration from the multicompartment model during one exhalation is plotted against exhaled volume. Vertical dashed lines represent 50% and 90%, respectively, of the total exhaled volume. C_{III} is the mean concentration of the gas in phase III. *C*: plot of normalized phase III slope vs. lung turnover to determine Sacin and Scond. Theoretical calculations demonstrate that the rate of increase in $S_{III_{N_2}}$ with lung turnover over the range of 1.5–6.0 provides an index of ventilation inhomogeneities in the proximal or conducting airways (airway generations 1–16). This index is denoted Scond (liters^{-1}). Furthermore, an index of ventilation inhomogeneity in the acinar region (airway generations 17–23) is denoted Sacin (liters^{-1}, magnitude of dark gray-shaded region) and can be extracted from $S_{III_{N_2}}$ in the first breath (after subtracting the component due to Scond − height of light-gray shaded region and equal to Scond multiplied by lung turnover for the first breath).

and equal to the atmospheric concentration. During the simulation, tidal volume is assumed to be 1 liter, and flow is saw tooth at ±200 ml/s with a period of 10 s (corresponding to slow deep tidal breathing at a respiratory rate of 6 breaths/min). Boundary conditions during inspiration are adjusted by accounting for the dilution of nitrogen within the alveolar compartments. During expiration, nitrogen concentrations are held fixed at the end-inspiration value. The entire washout is simulated and Sacin and Scond are calculated (Fig. 2). Model-simulated Sacin and Scond are matched to experimentally observed Sacin and Scond in healthy and asthmatic subjects by adjusting the values of the four structural and ventilation parameters using nonlinear regression. Thus we can determine a physiological range for these parameters in healthy and asthmatic subjects. Once the structural and ventilation parameters are determined, we can then simulate the exchange of NO by making the source term nonzero and reverting to the initial and boundary conditions in *Eq. 6*.

Experimental exhaled NO tracings. Experimental exhaled NO profiles were examined from a previous study investigating the effect of exercise-induced bronchoconstriction on exhaled NO in adults with mild asthma (24). This study enrolled nine subjects with mild exercise-induced bronchoconstriction who managed their symptoms with β-agonists (e.g., Albuterol) only. An inclusion criteria was >10% decrease in FEV_1 following the exercise challenge (10 min running on treadmill at 80% of maximum heart rate). The study focused on a single exhalation with a preexpiratory breathhold to characterize airway and alveolar NO parameters, but we also collected exhaled NO at a constant exhalation flow of 50 ml/s according to the guidelines of the American Thoracic Society, both before and after exercise challenge. Details of all nine subjects have been previously reported (24). The protocol was approved by the Institutional Review Board at the University of California, Irvine, and written informed consent was obtained for each subject. Six subjects were able to adequately complete the constant-flow exhalation at a target flow of 50 ml/s both pre- and post-exercise challenge, and these subjects can be summarized by the following indexes (mean ± SD): age, 30 ± 7 yr; height, 1.7 ± 0.12 m; weight, 78 ± 10 kg; Vaw, 178 ± 18 ml; FVC, 89 ± 14%predicted; FEV_1, 78 ± 18%predicted; FEV_1/FVC, 63 ± 11%; %change in FEV_1 following exercise challenge, 25 ± 17%. We did not previously present or analyze the NO tracings (NO concentration as a function of time or exhaled volume) at a constant flow of 50 ml/s.

For exhaled NO tracings, the fractional exhaled NO concentration, F_{ENO}, is plotted as a function of exhaled volume (Vex) normalized by an estimate of the subject's airway (dead space) volume (Vaw). In other words, the abscissa is airway volume turnover. The airway volume is estimated by the subject's ideal body weight in pounds plus age in years (3, 29) and thus accounts for variation in size of the subjects. The profile can then be characterized by three indexes consistent with previous reports (4, 30): *1*) the fractional concentration of phase III at a constant exhalation flow ($F_{ENO,\dot{V}}$), defined as the mean concentration over the window $2 < Vex/Vaw < 3$; *2*) the normalized phase III slope (S_{IIINO}), defined as the slope of the exhaled concentration over the window $2 < Vex/Vaw < 3$ divided by $F_{ENO,\dot{V}}$; and *3*) the rise volume ($V90_{NO}$), defined as the number of exhaled airway volumes needed to reach 90% of $F_{ENO,\dot{V}}$. In a similar fashion, the mean exhalation flow, $\dot{V}_{III}$, and normalized phase III slope of the flow, $S_{III\dot{V}}$, can also be defined over the window $2 < Vex/Vaw < 3$.

RESULTS

Experimental exhaled NO profiles. Experimental exhaled NO profiles from the six mild asthmatic subjects are shown in Fig. 3, *A–F*. Note that for each subject, the exhalation flow is constant near the target flow of 50 ml/s (Fig. 3*A*, *inset*) and does not change between baseline (58.0 ± 8.9 ml/s) and postexercise challenge (58.6 ± 12.2 ml/s). Exhaled NO profiles at baseline are generally characterized by an initial rapid rise in NO concentration ($Vex/Vaw < 2$) followed by a region that approaches a constant or plateau concentration ($Vex/Vaw > 2$). Baseline $F_{ENO,50}$ values for these subjects lie between 18 and 40 ppb with a mean (±SD) of 28 ± 7.8 ppb (Fig. 4*B*). Both $\bar{S}_{III\dot{V}}$ and $\bar{S}_{IIINO}$ are not statistically different from zero (−0.037 ± 0.031 and 0.0067 ± 0.056, respectively), and $V90_{NO}$ is 1.3 ± 0.26 (Fig. 4*C*).

Different patterns are observed after exercise challenge and can generally be characterized by a slower rise of the exhaled NO concentration with exhaled volume, resulting in a decrease in $F_{ENO,50}$ and a more positive slope in phase III of exhalation. Mean (±SD) for $F_{ENO,50}$, $\bar{S}_{III\dot{V}}$, S_{IIINO}, and $V90_{NO}$ after exercise challenge are 23 ± 8.1 ppb, 0.035 ± 0.044, 0.12 ± 0.066, and 1.8 ± 0.2, respectively, which are all statistically different from baseline. Of note, S_{IIINO} is statistically different from zero (positive), but $\bar{S}_{III\dot{V}}$ is not (Fig. 4, *D* and *E*).

Ventilation and structural parameters. MBNW simulations allow for quantification of the model ventilation and structural

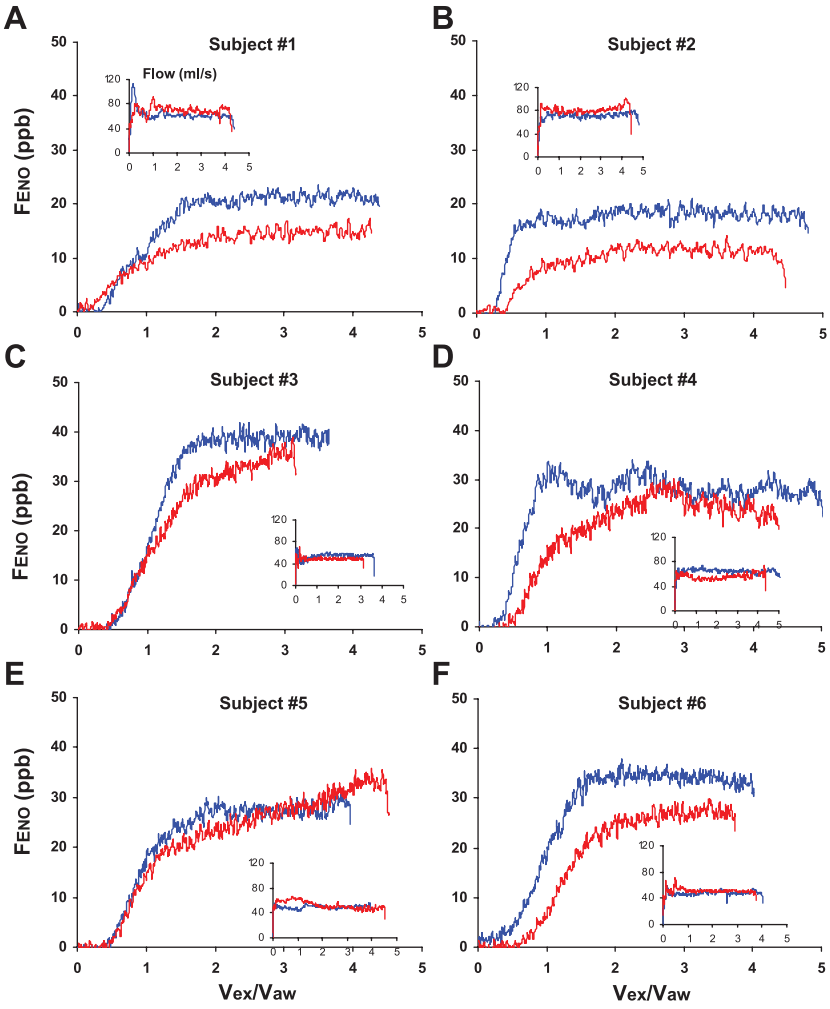

Fig. 3. Experimental NO tracings at constant exhalation flow preexercise (blue lines) and postexercise (red lines) for 6 subjects (*A–F*). *Insets* show exhalation flow for each maneuver. Each tracing represents the average of 2–3 consecutive maneuvers for each subject. The fractional exhaled NO concentration (F_{ENO}) is plotted as a function of exhaled volume (Vex) normalized by an estimate of the subject's airway (dead space) volume (Vaw).

parameters. Reported values of Sacin and Scond for both asthmatic and normal subjects were used to generate ventilation and structural parameters for four cases: healthy (Sacin = 0.068, Scond = 0.033), proximal airway heterogeneity (Sacin = 0.068, Scond = 0.060), peripheral airway heterogeneity (Sacin = 0.18, Scond = 0.033), and both proximal and peripheral heterogeneity (Sacin = 0.18, Scond = 0.06) (5, 35–37). We determined optimal values of ventilation and structural parameters (N, α, $\dot{V}_{1,0}$, and τ) for each of the three cases above (Table 1) using nonlinear regression to obtain the desired values of Scond and Sacin. These simulations were performed before simulating NO exchange. In addition, with the assumption of equal elastances in the two compartments, the steady-state flows in each compartment are equal. Figure 5, *A–C*, shows the flow through each airway compartment as a function of time for each condition (healthy, abnormal Sacin, abnormal Scond, and abnormal Sacin and Scond). In each case, the flow through *compartment 1* is always higher than that in *compartment 2*, and thus *compartment 1* represents the better ventilated region of the lung.

Model-simulated exhaled NO profiles. Exhaled NO profiles were simulated using the model geometry and ventilation parameters representative of healthy and abnormal ventilation distributions. Reasonable values for $J'aw_{NO}$ (1,100 pl/s) and $\bar{C}A_{NO}$ (3 ppb) where chosen on the basis of reports in the literature for healthy and asthmatic subjects as well as to achieve $F_{ENO,50}$ similar to that observed in our group of asthmatic subjects. The goal of the simulations was not to precisely replicate the experimental tracings but rather to simulate the major features (e.g., S_{IIINO}).

Figure 6*A* shows that when NO production is homogeneous (equal volume-weighted airway flux, equal alveolar concentrations), ventilation heterogeneity has only a small effect on the exhaled NO profiles. The healthy case results in a slightly negative phase III slope for NO ($S_{IIINO} = -0.002$), $F_{ENO,50} = 29.5$ ppb, and $V90_{NO} = 0.675$. When a greater degree of heterogeneity is present in either the conducting airways (abnormal Scond), the peripheral region (abnormal Sacin), or both (abnormal Sacin and Scond), there is essentially no change to the exhalation profile.

Figure 6, *B* and *C*, shows the effect of heterogeneous NO production in the airways and the alveolar regions, respectively, with healthy ventilation parameters. When 70% of $J'aw_{NO}$ is placed in the central compartment, $F_{ENO,50}$ increases 35% to 39.8 ppb compared with the homogeneous case, while a larger flux in one of the peripheral compartments results in a decrease of 11.5 and 8.4% in $F_{ENO,50}$ relative to the homogeneous case for *compartments 1* and *2*, respectively (Fig. 6*B*). S_{IIINO} is near zero for all three cases, but $V90_{NO}$ is increased when the NO flux is weighted in the poorly ventilated *com-*

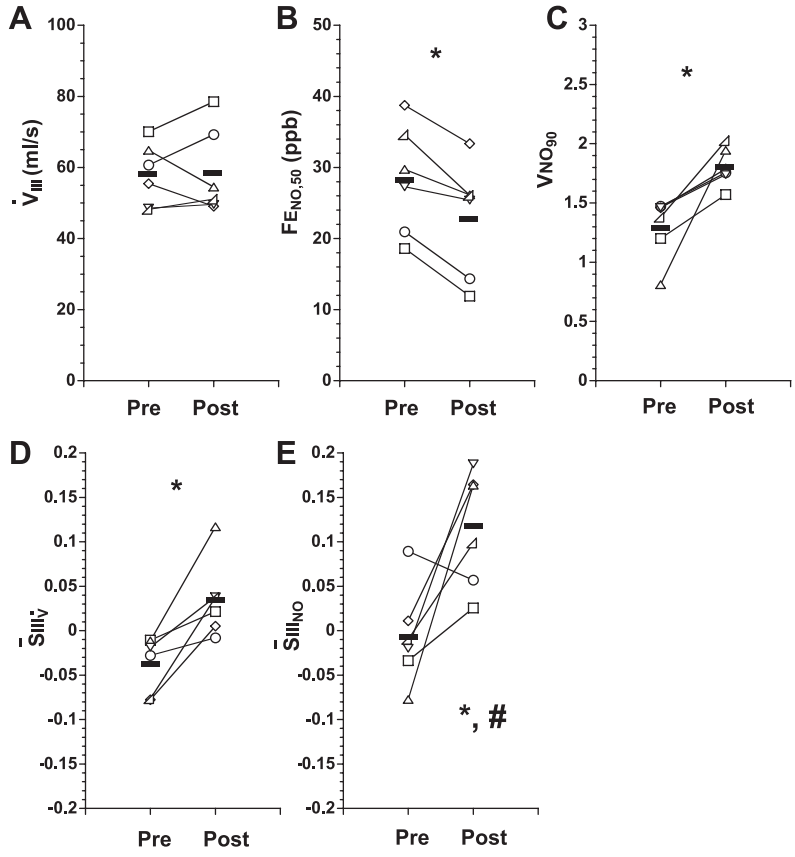

Fig. 4. Comparison of ventilation and NO exchange in each subject before (Pre) and after exercise challenge (Post). *A*: mean exhalation flow ($\dot{V}_{III}$). *B*: mean fractional concentration of NO at constant exhalation flow of 50 ml/s ($FE_{NO,50}$). *C*: normalized exhaled volume required to attain 90% of $FE_{NO,50}$ ($V90_{NO}$). *D*: normalized phase III slope of ventilation ($\bar{S}_{III\dot{V}}$). *E*: normalized phase III slope of NO ($\bar{S}_{III_{NO}}$). Pre- and postexercise values for each subject are denoted by the same open symbol and connected by a line. Thick horizontal bars show the mean values for each condition. *Significant difference compared with preexercise. #Significantly different from zero. Statistical significance determined by paired *t*-test ($P < 0.05$) between pre- and postexercise cases.

partment 2 ($V90_{NO} = 0.8$) and decreased when the NO flux is weighted in the central compartment ($V90_{NO} = 0.55$).

Figure 6*C* shows the effect of heterogeneous alveolar NO concentrations, which are modest. When the volume-weighted mean alveolar concentration is held constant (3 ppb), but the alveolar concentration is larger in the slow (and smaller) emptying compartment ($CA_{NO,1} = 0.94$, $CA_{NO,2} = 7.5$), $\bar{S}_{III_{NO}}$ becomes positive, $V90_{NO}$ increases (0.75), and there is a small 3.4% increase in $FE_{NO,50}$ (30.4 ppb). When the fast (and larger) emptying compartment has a larger concentration ($CA_{NO,1} = 4.14$, $CA_{NO,2} = 0.52$), the trends are the opposite: $\bar{S}_{III_{NO}}$ remains slightly negative, $V90_{NO}$ decreases (0.625), and $FE_{NO,50}$ decreases slightly (1.9% to 29 ppb).

Figure 6, *D* and *E*, shows the combined effects of heterogeneity in ventilation and NO production. Although there are many possible combinations, we focused on five illustrative cases that are consistent with the pathophysiology of asthma. Figure 6*D* combines lower airway ventilation heterogeneity (abnormal Sacin) with either an increased NO airway flux or an increased alveolar concentration in the slower-emptying branch of the model (*compartment 2*). Figure 6*E* combines proximal ventilation heterogeneity (abnormal Scond) with an increased NO flux in either the central compartment or the slow-emptying compartment. Figure 6*E* also includes a simulated tracing for abnormal Sacin and Scond with an increased flux and alveolar concentration in the slow-emptying branch. The latter case simulates global ventilation and inflammation heterogeneity.

Peripheral ventilation heterogeneity with enhanced alveolar NO tends to create a positive $\bar{S}_{III_{NO}}$ (0.013) with a small increase in $FE_{NO,50}$ (30.3 ppb). In contrast, peripheral ventilation heterogeneity with enhanced lower airway NO flux sig-

Table 1. *Ventilation parameters*

	Healthy (Sacin = 0.068; Scond = 0.033	Abnormal Sacin (Sacin = 0.18; Scond = 0.033)	Abnormal Scond (Sacin = 0.068; Scond = 0.06)	Abnormal Scond and Sacin (Sacin = 0.18; Scond = 0.06)
$\dot{V}_{1,0}/\dot{V}$	0.85	0.95	0.95	0.99
$\dot{V}_{1,\infty}/\dot{V}$	0.5	0.5	0.5	0.5
$\tau/(Vaw/\dot{V})$	1.02	1.92	1.04	2.11
α	0.69	0.73	0.61	0.68
N	7	7	7	7
Vaw, ml	181	181	181	181
Vaw_0, ml	51	51	51	51
Vaw_1, ml	89	95	80	88
Vaw_2, ml	41	35	50	42

See *Glossary* for definitions.

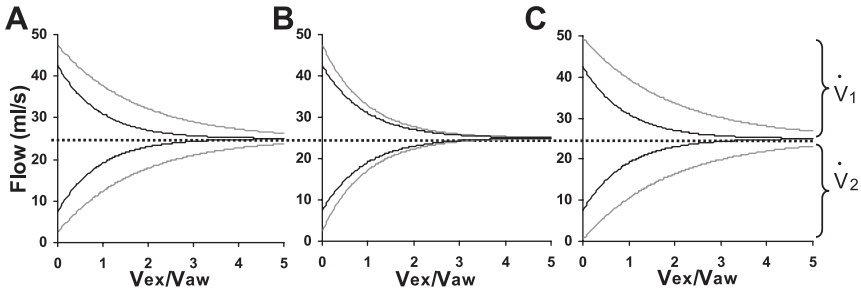

Fig. 5. Exhalation flow through each airway compartment as a function of time for different structural and ventilation parameters. In *A–C*, healthy ventilation (Sacin = 0.068, Scond = 0.033) is shown as a solid black line. *A*: enhanced heterogeneity in the peripheral conducting airways and alveolar region (Sacin = 0.18, Scond = 0.033). *B*: enhanced heterogeneity in the proximal airways (Sacin = 0.068, Scond = 0.06). *C*: enhanced heterogeneity in both the proximal and peripheral regions of the lungs (Sacin = 0.18, Scond = 0.033). In each case the total flow through the central airway compartment is held constant at 50 ml/s. $\dot{V}_1$ and $\dot{V}_2$ are flow in airway *compartments 1* and *2*, respectively.

nificantly right-shifts the profile ($V90_{NO}$ increases to 0.95), enhances $S_{III_{NO}}$ further (0.017), but decreases $FE_{NO,50}$ by 8.9% (26.9 ppb). Proximal ventilation heterogeneity with NO airway flux weighted in the central compartment significantly enhances $FE_{NO,50}$ (39.8 ppb) and reduces $V90_{NO}$ (0.525). When the NO flux is weighted in the peripheral *compartment 2*, $FE_{NO,50}$ is reduced by 10.4% and right-shifted ($V90_{NO}$ = 0.875). The most significant effect is observed when both proximal and peripheral ventilation are abnormal, and both the NO airway flux and alveolar concentration are enhanced in *compartment 2*. For this case, $FE_{NO,50}$ is reduced by 11% (26.2 ppb), and the profile is significantly right-shifted ($V90_{NO}$ = 1.18) with a significant positive $S_{III_{NO}}$ (0.04).

DISCUSSION

Exhaled NO profiles from asthmatic subjects may reach a plateau concentration at a steady exhalation flow but may also increase or decrease with exhaled volume. The latter observations may be due to localized inflammation and ventilation heterogeneity. Current theoretical models of NO dynamics in the lungs utilize a single-path trumpet shape that partitions the exhaled concentration into one airway and one alveolar contribution and thus, at a constant exhalation flow, predict only a constant exhaled NO concentration. In this study we developed a simple multicompartment model to demonstrate that spatial heterogeneity in NO production and ventilation can significantly impact the exhaled NO profile in patterns that are consistent with those observed experimentally in exercise-induced asthma.

Effect of ventilation and NO production heterogeneity. The primary aim of the present study is to illustrate the effect of spatial heterogeneity in ventilation and NO production on exhaled NO dynamics using a simple model. Our results show that the exhaled NO profile is strongly affected by the interplay between structure, ventilation (flow), and NO production.

Both experimental and simulated exhaled NO tracings can be characterized by two phases: *1*) a dynamic phase, corresponding to phases I and II of the classic tracing from an inert gas such as N_2, in which the exhaled concentration is changing rapidly with time or exhaled volume (characterized by $V90_{NO}$); and *2*) a nearly steady-state phase, corresponding to phase III of an inert gas profile, in which the exhaled concentration approaches a constant (or plateau) value (characterized by $FE_{NO,\dot{V}}$ and $S_{III_{NO}}$). The dynamic phase is due to three factors. First, the initial airway compartment that is emptied (Vex/Vaw $<$ 1) has a steep axial gradient of NO beginning with inspired air of zero NO at the mouth and increasing with z-position due to the increased residence time during inspiration. Second, the flow in each compartment is changing in time with a characteristic time constant, τ, that captures the resistance of the alveolar and airway regions (Table 1 and Fig. 5). Third, while the airway flux is assumed constant for flows $>$ 50 ml/s, the axial (z position) gradient in NO concentration, which describes axial diffusion of NO (see *Eq. 1*), is changing in time.

Heterogeneous flow with uniform NO production had only a minimal impact on the exhalation profile of NO. When total flow is held constant, the contribution of the airways to the exhaled concentration is directly related to the residence time of the air within the airway compartment (recall the airway flux in each compartment is an amount of NO per unit time). At early times in Fig. 6 (Vex/Vaw $<$ 0.5), the exhaled NO signal represents the contribution of the central airways (*compartment 0*). Since the volume and flow, and hence residence time, in this compartment are identical for the three cases, the tracings overlap. At later times the exhaled air consists of a mixture from *compartments 1* and *2*, whose effective residence time is a flow-weighted combination of residence times in the individual compartments. Differences between the three cases for 0.5 $<$ Vex/Vaw $<$ 3 represent the temporal variation of flows in *compartments 1* and *2*, and hence effective residence time, in this period (see Fig. 5). Once flow in each compartment is constant (Vex/Vaw $>$ 3), the effective residence time of exhaled air also remains constant, and any further changes in the exhaled concentration with time or exhaled volume are due to changes in the axial gradient.

In contrast to ventilation, NO production heterogeneity had a significant impact on exhaled NO profiles. Different airway fluxes were assigned to different compartments while holding the total airway flux constant. A compartment with a higher flux compared with the homogeneous case could represent a locally inflamed region. This condition resulted in significant alterations to the plateau concentration of NO. When the higher flux was localized to the central airway compartment, the plateau concentration was significantly increased. In contrast, when the higher flux was localized in one of the lower compartments, the plateau concentration was reduced to varying degrees. When the total NO flux is homogeneously distributed, the magnitude of the source term ($J'aw_{NO,i}$/Vaw, flux of NO per unit airway volume) in *Eq. 1* is identical in all three

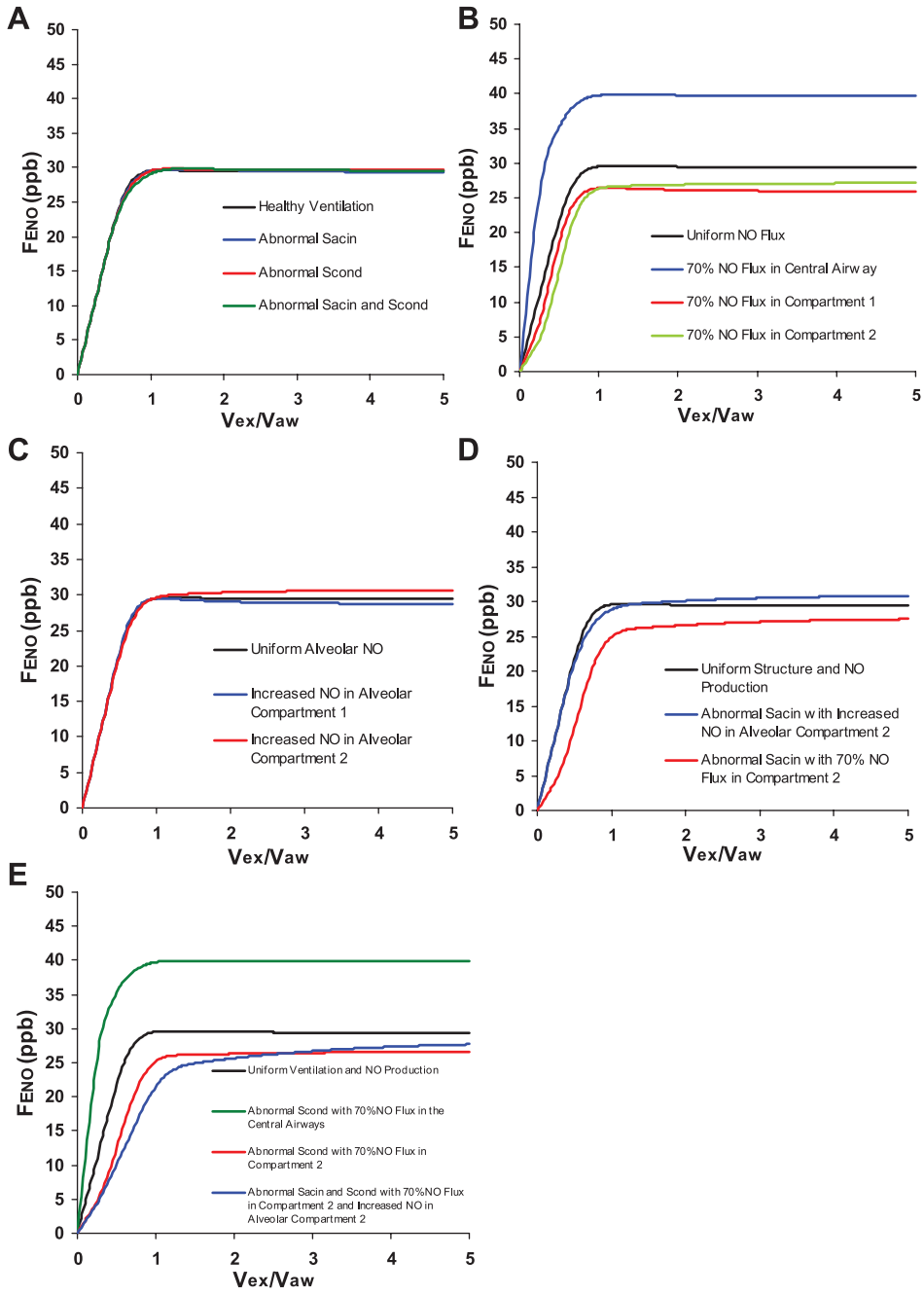

Fig. 6. Effect of ventilation and NO production heterogeneity on exhaled NO profiles using the multicompartment model. *A*: ventilation heterogeneity (abnormal Sacin and/or Scond) with homogeneous NO production. *B*: heterogeneous NO production in the airway (healthy ventilation). *C*: heterogeneous alveolar concentrations (healthy ventilation). *D*: heterogeneous airway NO production or alveolar NO combined with peripheral ventilation heterogeneity (abnormal Sacin). *E*: heterogeneous airway NO production or alveolar NO combined with proximal ventilation heterogeneity (abnormal Scond), as well as global NO production and ventilation heterogeneity. In each case, the exhalation profile representing uniform NO production and healthy ventilation is shown in black.

airway compartments. When the fraction of the flux assigned to a particular compartment is larger than its fraction of the total airway volume, the source term is disproportionately increased in this compartment and results in a higher NO flux within that compartment. Since the total flux is held constant, this increase is offset by corresponding decreases in the fluxes in the other compartments. However, the contribution of a compartment to the overall exhaled NO depends both on the NO source within that compartment and the flow through it. For example, a compartment with a large source term but zero flow would not contribute to the exhaled NO.

To explain the effect of different spatial flux distributions, we define a flow-weighted average NO source for the whole airway tree as the sum of the source terms in each compartment weighted by the exhalation flow in each compartment: $J'aw_{NO} = \Sigma_{i=0}^{2} (J'aw_{NO,i}/Vaw_i) \times (\dot{V}_i/\dot{V})$. When the NO flux is homogeneously distributed ($J'aw_{NO,i}/Vaw_i$ = constant), this quantity is equal to $2 \times J'aw_{NO}/Vaw$, i.e. two times the flux per unit volume of the airway tree. The factor of 2 accounts for the serial nature of the flow between the lower and central compartments.

First consider the case when 70% of the total flux is localized in the central compartment. As the volume of the central compartment (51 ml) represents only 28% of the total airway volume, the flux per unit volume is increased by 150%. Since all the exhaled air passes through this compartment ($\dot{V} = \dot{V}_1 + \dot{V}_2$), there is a net increase of 150% in the contribution of the central compartment to $J'aw_{NO}$. This increase is offset

by corresponding decreases of the contributions from *compartments 1* and *2*. However, the net effect is a 46% increase in $\bar{J}'aw_{NO}$ compared with the homogeneous case. In contrast, when 70% of the flux is localized in *compartments 1* or *2*, similar calculations show that $\bar{J}'aw_{NO}$ is reduced by 11% and 14%, respectively. Thus the magnitude of the decrease depends on the relative flux per unit volume and flows in each compartment. This reasoning does not precisely explain the magnitude of change in $F_{ENO,50}$ when the NO flux is spatially heterogeneous. For instance, when the higher flux is localized in the central compartment, $F_{ENO,50}$ increases by 35% while $\bar{J}'aw_{NO}$ increases by 46%. This is a result of neglecting axial diffusion in defining the effective NO source. Axial diffusion would tend to make the spatial NO concentrations more homogeneous and thus reduce the magnitude of changes compared with the homogeneous case. Nonetheless, this reasoning provides an intuitive explanation of the direction of changes in $F_{ENO,50}$ when the NO flux is spatially heterogeneous.

Distributing the total alveolar concentration heterogeneously has only a modest impact on the exhalation NO profile in these simulations due primarily to the relative contribution (1–8 ppb) of the alveolar NO to F_{ENO} (~30 ppb). However, if an inflamed peripheral region (higher alveolar NO concentration) empties slower, the exhaled NO concentration will tend to increase with exhaled volume, creating a positive S_{IIINO}.

The most significant changes in the exhaled NO profile are observed when both NO production and ventilation are heterogeneous. This physiological condition might occur if an inflamed region enhances the production of NO, but also results in bronchoconstriction, thus reducing ventilation. The underlying mechanisms are the same as that discussed for isolated heterogeneity in flow and NO production; that is, the plateau concentration will depend on the relative weighting of the total airway NO flux per unit volume and flow within the airway compartments. Since ventilation is also heterogeneous, there is a larger range of residence times, and thus a larger range of plateau concentrations. For example, when Scond is abnormal, only 5% of the flow (2.5 ml/s) at steady state is in *compartment 2* (Table 1). Hence, when 70% of the total airway NO flux is placed in this compartment, the result is a significant decrease in the plateau concentration (Fig. 5*D*).

All of the experimental asthmatic profiles in Fig. 3 have a positive S_{IIINO} postexercise, resulting in a delay in the appearance of NO (increased $V90_{NO}$) and decrease in $F_{ENO,50}$. Our model indicates this scenario is consistent with ventilation heterogeneity in either the proximal or peripheral airway combined with enhanced NO airway flux in the slower emptying compartment relative to the remaining lung. The enhanced heterogeneity in NO production may be due to the enhanced rate of ventilation during exercise, which would preferentially washout NO stores in well-ventilated airways, resulting in a higher NO flux in the poorly ventilated region. Note that these observations cannot be explained with single-path models that utilize a single airway compartment and a single homogeneous alveolar region.

The multicompartment model represents the simplest generalization of the existing two-compartment model of pulmonary NO exchange (4, 23, 28) that could incorporate ventilation heterogeneity by considering two airway compartments that empty at different rates. This model for asthma is characterized by four independent structural and ventilation parameters (*N*, α, τ, and $\dot{V}_{1,0}$), whose values were chosen to generate reasonable values for Sacin and Scond in healthy and asthmatic lungs. The set of values for the structural and ventilation parameters are not unique but do represent values that are physiological. Thus, although a different set of ventilation and structural parameters could have been chosen, the simulations represent a realistic prediction of how ventilation and NO production heterogeneity can impact the exhaled NO profile. Further, the results indicate that incorporating information about ventilation heterogeneity obtained from multiple-breath nitrogen washout into models of NO exchange dynamics may improve the interpretation of exhaled NO profiles. Although beyond the scope of the present study, future studies may describe a more rigorous approach to determine the structural and ventilation parameters for each subject on the basis of nonlinear regression techniques to fit the model MBNW profiles to experimental tracings. A similar approach might be employed to determine unique and subject-specific values for the five NO production parameters.

In conclusion, we have developed the first model of pulmonary NO exchange that incorporates heterogeneity in ventilation and NO production. Model simulations suggest that the combination of ventilation and NO production heterogeneity may significantly affect the magnitude and shape of exhaled NO profiles in patterns that are consistent with experimental observations in mild asthmatic subjects following an exercise challenge. This result confounds the interpretation of the plateau NO concentration. Hence, characterizing NO exchange dynamics with region-specific alveolar NO concentrations and airway flux of NO in the multicompartment model may provide more useful physiological information than either plateau concentration alone, or an airway flux and alveolar concentration from the single-path, two-compartment model.

ACKNOWLEDGMENTS

We thank the General Clinical Research Center at University of California, Irvine.

GRANTS

This work was supported by National Institutes of Health Grants HL-070645 and RR-00827.

REFERENCES

1. **Alving K, Weitzberg E, Lundberg JM.** Increased amount of nitric oxide in exhaled air of asthmatics. *Eur Respir J* 6: 1368–1370, 1993.
2. **Bates JH, Rossi A, Milic-Emili J.** Analysis of the behavior of the respiratory system with constant inspiratory flow. *J Appl Physiol* 58: 1840–1848, 1985.
3. **Bouhuys A.** Respiratory dead space. In: *Handbook of Physiology. Respiration.* Washington, DC: Am. Physiol. Soc, 1964, sect. 3, chapt. 28, p. 699–714.
4. **Condorelli P, Shin HW, Aledia AS, Silkoff PE, George SC.** A simple technique to characterize proximal and peripheral nitric oxide exchange using constant flow exhalations and an axial diffusion model. *J Appl Physiol* 102: 417–425, 2007.
5. **Downie SR, Salome CM, Verbanck S, Thompson B, Berend N, King GG.** Ventilation heterogeneity is a major determinant of airway hyperresponsiveness in asthma, independent of airway inflammation. *Thorax* 62: 684–689, 2007.
6. **Gelb AF, Taylor CF, Nussbaum E, Gutierrez C, Schein A, Shinar CM, Schein MJ, Epstein JD, Zamel N.** Alveolar and airway sites of nitric oxide inflammation in treated asthmatics. *Am J Respir Crit Care Med* 170: 737–741, 2004.
7. **Gustafsson PM, Ljungberg HK, Kjellman B.** Peripheral airway involvement in asthma assessed by single-breath SF6 and He washout. *Eur Respir J* 21: 1033–1039, 2003.

8. **Hogman M, Drca N, Ehrstedt C, Merilainen P.** Exhaled nitric oxide partitioned into alveolar, lower airways and nasal contributions. *Respir Med* 94: 985–991, 2000.
9. **Lehtimaki L, Kankaanranta H, Saarelainen S, Turjanmaa V, Moilanen E.** Increased alveolar nitric oxide concentration in asthmatic patients with nocturnal symptoms. *Eur Respir J* 20: 841–845, 2002.
10. **Lehtimaki L, Kankaanranta H, Saarelainen S, Turjanmaa V, Moilanen E.** Peripheral inflammation in patients with asthmatic symptoms but normal lung function. *J Asthma* 42: 605–609, 2005.
11. **Mattes J, Storm van's Gravesande K, Reining U, Alving K, Ihorst G, Henschen M, Kuehr J.** NO in exhaled air is correlated with markers of eosinophilic airway inflammation in corticosteroid-dependent childhood asthma. *Eur Respir J* 13: 1391–1395, 1999.
12. **Paiva M.** Two new pulmonary functional indexes suggested by a simple mathematical model. *Respiration* 32: 389–403, 1975.
13. **Paiva M, Engel LA.** The anatomical basis for the sloping N_2 plateau. *Respir Physiol* 44: 325–337, 1981.
14. **Paiva M, Engel LA.** Theoretical studies of gas mixing and ventilation distribution in the lung. *Physiol Rev* 67: 750–796, 1987.
15. **Paiva M, van Muylem A, Engel LA.** Slope of phase III in multibreath nitrogen washout and washin. *Bull Eur Physiopath Respir* 18: 273–280, 1982.
16. **Paiva M, Verbanck S, van Muylem A.** Diffusion-dependent contribution to the slope of the alveolar plateau. *Respir Physiol* 72: 257–270, 1988.
17. **Paraskakis E, Brindicci C, Fleming L, Krol R, Kharitonov SA, Wilson NM, Barnes PJ, Bush A.** Measurement of bronchial and alveolar nitric oxide production in normal children and children with asthma. *Am J Respir Crit Care Med* 174: 260–267, 2006.
18. **Persson MG, Wiklund NP, Gustafsson LE.** Endogenous nitric oxide in single exhalations and the change during exercise. *Am Rev Respir Dis* 148: 1210–1214, 1993.
19. **Pietropaoli AP, Perillo IB, Torres A, Perkins PT, Frasier LM, Utell MJ, Frampton MW, Hyde RW.** Simultaneous measurement of nitric oxide production by conducting and alveolar airways of humans. *J Appl Physiol* 87: 1532–1542, 1999.
20. **Schedin U, Frostell C, Persson MG, Jakobsson J, Andersson G, Gustafsson LE.** Contribution from upper and lower airways to exhaled endogenous nitric oxide in humans. *Acta Anaesthesiol Scand* 39: 327–332, 1995.
21. **Shin HW, Rose-Gottron CM, Cooper DM, Newcomb RL, George SC.** Airway diffusing capacity of nitric oxide and steroid therapy in asthma. *J Appl Physiol* 96: 65–75, 2004.
22. **Shin HW, Rose-Gottron CM, Perez F, Cooper DM, Wilson AF, George SC.** Flow-independent nitric oxide exchange parameters in healthy adults. *J Appl Physiol* 91: 2173–2181, 2001.
23. **Shin HW, George SC.** Impact of axial diffusion on nitric oxide exchange in the lungs. *J Appl Physiol* 93: 2070–2080, 2002.
24. **Shin HW, Schwindt CD, Aledia AS, Rose-Gottron CM, Larson JK, Newcomb RL, Cooper DM, George SC.** Exercise-induced bronchoconstriction alters airway nitric oxide exchange in a pattern distinct from spirometry. *Am J Physiol Regul Integr Comp Physiol* 291: R1741–R1748, 2006.
25. **Silkoff PE, McClean PA, Slutsky AS, Furlott HG, Hoffstein E, Wakita S, Chapman KR, Szalai JP, Zamel N.** Marked flow-dependence of exhaled nitric oxide using a new technique to exclude nasal nitric oxide. *Am J Respir Crit Care Med* 155: 260–267, 1997.
26. **Silkoff PE, Sylvester JT, Zamel N, Permutt S.** Airway nitric oxide diffusion in asthma. Role in pulmonary function and bronchial responsiveness. *Am J Respir Crit Care Med* 161: 1218–1228, 2000.
27. **Tgavalekos NT, Tawhai M, Harris RS, Musch G, Vidal-Melo M, Venegas JG, Lutchen KR.** Identifying airways responsible for heterogeneous ventilation and mechanical dysfunction in asthma: an image functional modeling approach. *J Appl Physiol* 99: 2388–2397, 2005.
28. **Tsoukias NM, George SC.** A two-compartment model of pulmonary nitric oxide exchange dynamics. *J Appl Physiol* 85: 653–666, 1998.
29. **Tsoukias NM, Shin HW, Wilson AF, George SC.** A single-breath technique with variable flow rate to characterize nitric oxide exchange dynamics in the lungs. *J Appl Physiol* 91: 477–487, 2001.
30. **Tsoukias NM, Tannous Z, Wilson AF, George SC.** Single-exhalation profiles of NO and CO_2 in humans: effect of dynamically changing flow rate. *J Appl Physiol* 85: 642–652, 1998.
31. **Van Muylem A, Noel C, Paiva M.** Modeling of impact of gas molecular diffusion on nitric oxide expired profile. *J Appl Physiol* 94: 119–127, 2003.
32. **Venegas JG, Schroeder T, Harris S, Winkler RT, Melo MF.** The distribution of ventilation during bronchoconstriction is patchy and bimodal: a PET imaging study. *Respir Physiol Neurobiol* 148: 57–64, 2005.
33. **Venegas JG, Winkler T, Musch G, Vidal Melo MF, Layfield D, Tgavalekos N, Fischman AJ, Callahan RJ, Bellani G, Harris RS.** Self-organized patchiness in asthma as a prelude to catastrophic shifts. *Nature* 434: 777–782, 2005.
34. **Verbanck S, Paiva M.** Model simulations of gas mixing and ventilation distribution in the human lung. *J Appl Physiol* 69: 2269–2279, 1990.
35. **Verbanck S, Schuermans D, Noppen M, Van Muylem A, Paiva M, Vincken W.** Evidence of acinar airway involvement in asthma. *Am J Respir Crit Care Med* 159: 1545–1550, 1999.
36. **Verbanck S, Schuermans D, Paiva M, Vincken W.** The functional benefit of anti-inflammatory aerosols in the lung periphery. *J Allergy Clin Immunol* 118: 340–346, 2006.
37. **Verbanck S, Schuermans D, Van Muylem A, Paiva M, Noppen M, Vincken W.** Ventilation distribution during histamine provocation. *J Appl Physiol* 83: 1907–1916, 1997.
38. **Weibel E.** *Morphometry of the Human Lung*. Berlin, Germany: Springler-Verlag, 1963.